

# Tribological properties of MgZrO<sub>3</sub> coatings deposited by plasma spraying

Y. Y. Özbek<sup>1\*</sup>, V. Uçar<sup>2</sup>, A. Ş. Demirkiran<sup>1</sup>

<sup>1</sup>*Department of Metallurgical and Materials Science, Engineering Faculty, Sakarya University, Esentepe Campus, 54187 Sakarya, Turkey*

<sup>2</sup>*Department of Mechanical Engineering, Engineering Faculty, Sakarya University, Esentepe Campus, 54187 Sakarya, Turkey*

Received 22 February 2007, received in revised form 3 May 2007, accepted 4 July 2007

## Abstract

Because of thermal barrier properties, ceramic-based coatings are widely used for the design of components at high temperature applications. Therefore, 304 L stainless steel substrates were coated with MgZrO<sub>3</sub> coatings using atmospheric plasma spray technique. These coatings consist of a transition from the metallic bond layer to cermet and from cermet to the ceramic layer. Produced samples were characterized by optical microscope, scanning electron microscope and X-ray diffraction techniques. Wear tests were carried out in ball-on-disc system at ambient and dry friction conditions under 2 N load for 0.1, 0.15 and 0.2 m s<sup>-1</sup> sliding speeds. The results showed that the friction coefficient values changed between 0.250 and 0.259 depending on sliding speed. The specific wear rate values rise also from 3.4470 to 5.5535 × 10<sup>-3</sup> mm<sup>3</sup> N<sup>-1</sup> m<sup>-1</sup> with increasing sliding speed. Detailed examination of formed wear tracks on sample surfaces showed plastic deformation, materials transfer and microcracks.

**Key words:** tribology, wear, friction, plasma spray, MgZrO<sub>3</sub> coatings

## 1. Introduction

Surface engineering is an economic method used at the production of materials, tools and machine parts to improve surface properties, such as wear and corrosion resistance [1]. Plasma spray technology takes also part among surface engineering methods. Plasma sprayed ceramic coatings have been widely used in many industrial fields such as automotive, aerospace, aircraft because of an excellent wear, erosion, heat, oxidation and corrosion properties [2–5].

Compared with metallic and polymeric materials, ceramic materials have many advantages such as high hardness, high resistance to thermal and corrosive conditions and relatively low densities [5]. In recent years, researches have especially focused on the use of ZrO<sub>2</sub> based ceramic coatings as thermal barrier coatings [6]. Although zirconia possesses a low thermal conductivity and a suitable expansion match with the substrate, to use zirconia to its full potential, the polymorphism of zirconia necessitates stabilizing with other oxides.

Three crystal forms exist in ZrO<sub>2</sub> ceramics, namely the cubic, tetragonal and monoclinic structures in slowly decreasing order of temperature. The strength and toughness of the ceramics are closely related to the structures resulting from these transformations. The improvement related to the tetragonal to monoclinic transformation has been explained in terms of formation of a microcrack zone in front of the propagating crack. These microcracks form due to the strains associated with tetragonal to monoclinic transformation and toughen the materials by blunting the tip of the microcrack [7]. It can be suppressed by adding appropriate amounts of phase stabilizing oxides such as Y<sub>2</sub>O<sub>3</sub> (small content of yttrium increases the service life of the bond coat), CaO and MgO to zirconia ceramics [8–11].

Wear and friction are very important parameters causing tremendous losses at materials [12]. The friction and wear characteristics of plasma sprayed ZrO<sub>2</sub> based coatings are greatly affected by compositional and microstructural features, such as micro-

\*Corresponding author: tel.: +90 264 2955619; fax: +90 264 2955601; e-mail address: [yvarali@sakarya.edu.tr](mailto:yvarali@sakarya.edu.tr)

cracks, porosity, morphology, grain size, hardness and distribution of additions. The wear mechanisms of  $ZrO_2$  based ceramic coatings are complicated but can be classified by one of two dominant processes—brittle fracture or deformation with the change of wear conditions such as load, sliding speed and temperature, etc., the transition from fracture-dominated wear to deformation-dominated wear is often accompanied by great change in both friction and wear [6, 13].

In this study, wear behaviour of  $MgZrO_3$  coatings produced on AISI 304 L stainless steel substrates by plasma spray technique had been investigated. Wear tests were carried out using WC-Co ball using a ball-on-disc system at ambient and dry friction conditions under 2 N load with 0.1, 0.15 and 0.2  $m\ s^{-1}$  sliding speeds.

## 2. Experimental procedure

The powders produced by Metco Firm were used in these experiments. NiCrAl (Metco 443 NS) for bond coat and magnesia partially stabilized zirconia powders (Metco 210 NS) for top coat powders were chosen. Some properties such as particle sizes, compositions and melting points of using powders for coatings are shown in Table 1. SEM morphologies of the powders are shown in Fig. 1. NiCrAl powders are near-spherical (Fig. 1a), while  $MgZrO_3$  powders are irregular and angular (Fig. 1b). The substrate material is stainless steel AISI 304 L that is machined into  $\varnothing 30 \times 8$  mm in the form of circular plates. The chemical composition of the substrate is shown in Table 2.

The powders were dried before coating at temperature of 110 °C in a drying oven. Pre-treatment of substrates was performed by applying grit-blasting using 35 mesh  $Al_2O_3$ , followed by ultrasonic cleaning. Coatings were produced using an atmospheric plasma spray system, type Metco 3MB. A distance of 100–150 mm was selected between the gun and substrate during deposition of the powders. The graded coatings were used in order to reduce the mismatch effect, thermal expansion and interfacial stresses. Spray parameters recommended by Metco Firm were applied to produce coatings via plasma spray process. Different spraying conditions were used for each layer. The used spraying conditions were summarized in Table 3. The coatings were produced as follows: Grit-blasted substrates were first coated with a bond layer using 100 wt.% NiCrAl powders. On this bond layer 70 wt.% NiCrAl + 30 wt.%  $MgZrO_3$ , 50 wt.% NiCrAl + 50 wt.%  $MgZrO_3$ , 30 wt.% NiCrAl + 70 wt.%  $MgZrO_3$  powder mixtures were then coated as intermediate layers. At last, a top coat was produced using 100 wt.%  $MgZrO_3$  powders. Figure 2 shows a schematic representation of graded coatings obtained by using an atmospheric plasma spray system.

Table 1. Some properties of powders

Coating powders	Composition (wt.%)	Particle size ( $\mu m$ )	Melting point ( $^{\circ}C$ )	
MgZrO <sub>3</sub>	ZrO <sub>2</sub>	76	–100 + 40	2140
	MgO	22		
	HfO	1.5		
	CaO	0.5		
NiCrAl	Ni	72	–125 + 44	1420
	Cr	18		
	Al	6		
	Mn	1		
	Si	1		
	Fe	1		
	Organic binder	1		

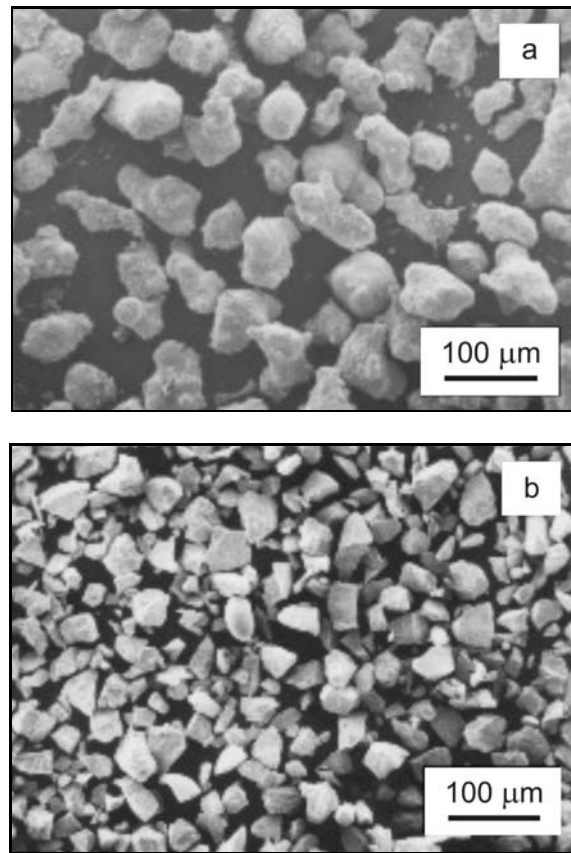


Fig. 1. SEM micrographs of powders: (a) NiCrAl and (b)  $MgZrO_3$ .

The crystal structures of the top coat were examined by a X-ray diffractometer (Phillips) operating with  $Co\ K\alpha$  ( $\lambda = 1.7902\ \text{\AA}$ ) radiation. The scanning electron microscopy (Phillips 525) was used to observe the morphologies of both powders and the coatings.

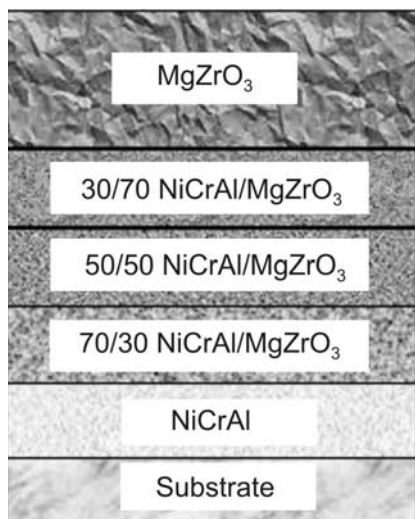


Fig. 2. Configuration of coatings produced by using an atmospheric plasma system.

The surface roughness of samples was measured using Mahr Perthometer M1.

After characterization, wear tests were conducted with a cemented carbide (WC-Co) ball with 4.6 mm in diameter sliding against plasma sprayed coatings. The wear tests were performed in ambient air and relative humidity ( $35 \pm 5$  % RH) and  $25 \pm 3$  °C. Schematic diagram of the ball-on-disc system is shown in Fig. 3. 2 N loads and 0.1, 0.15 and 0.2 m s<sup>-1</sup> sliding speeds were used at the wear tests. A sliding distance of 500 m was chosen. Microstructural observations were performed using scanning electron microscopy (SEM). The cross-section area of wear track,  $A$ , was determined using a surface profilometer. The standard deviation on a specimen was typically less than 10 percent of its average value. The wear volume,  $V_d$ , is calculated using:

$$V_d = 2\pi r A. \quad (1)$$

Here,  $r$  is the radius of the wear track [14].

### 3. Results and discussion

The high temperature reached in plasma spray sys-

Table 2. Chemical composition of substrate

	Elements									
	C	Si	Mn	Cr	Ni	Mo	Co	W	Cu	Fe
Composition (wt.%)	< 0.003	0.33	1.589	16.68	10.99	2.232	0.100	0.035	0.231	Balance

Table 3. Spray parameters applied in coating process

Spray parameters	Ar/H <sub>2</sub> (%)	Volt/Ampere	Spray distance (mm)	Gas pressure (Ar/H <sub>2</sub> )
100 % NiCrAl	80/20	60/500	125–150	10/40
70 % NiCrAl + MgZrO <sub>3</sub>	80/20	58/500	125–150	10/40
50 % NiCrAl + MgZrO <sub>3</sub>	80/15	54/500	125–150	150/40
30 % NiCrAl + MgZrO <sub>3</sub>	80/15	54/500	125–150	150/40
100 % MgZrO <sub>3</sub>	80/15	54/500	125–150	150/40

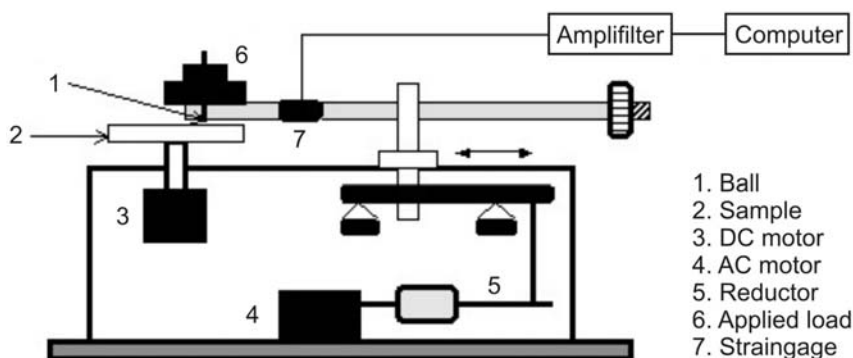


Fig. 3. Schematic illustration of the ball-on-disc wear system.

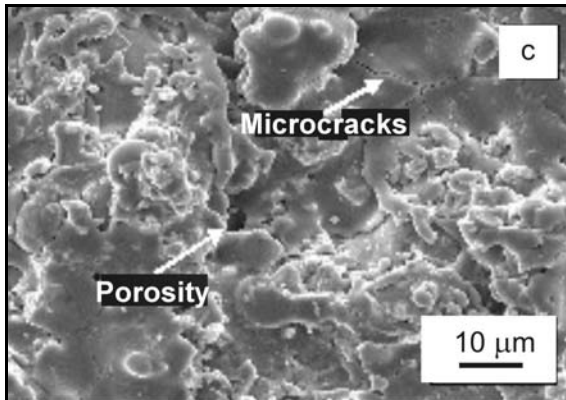
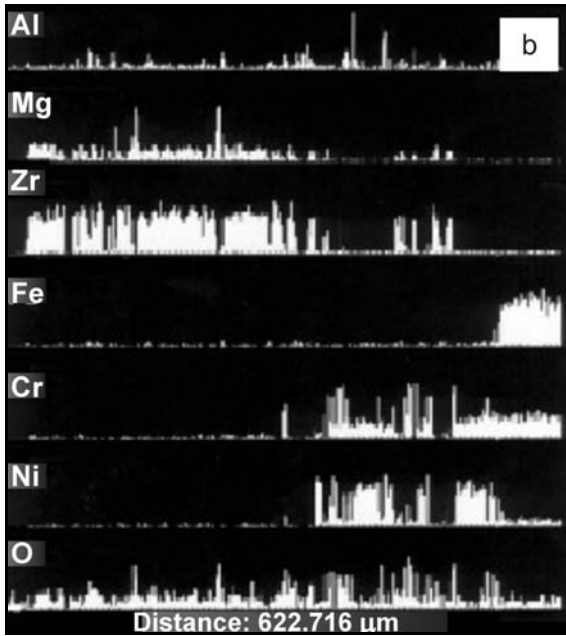
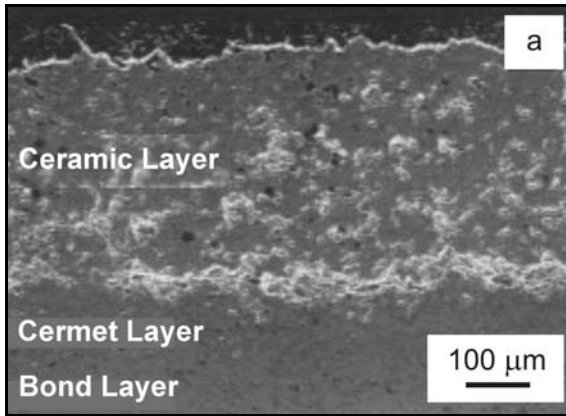


Fig. 4. (a) Cross-section SEM micrograph of coating, (b) EDS analysis through coating layer, (c) surface SEM micrograph of coatings.

tem allows melting of any materials within a very short time and leads to rough surface for as-sprayed coatings. These coatings consist of a transition from the

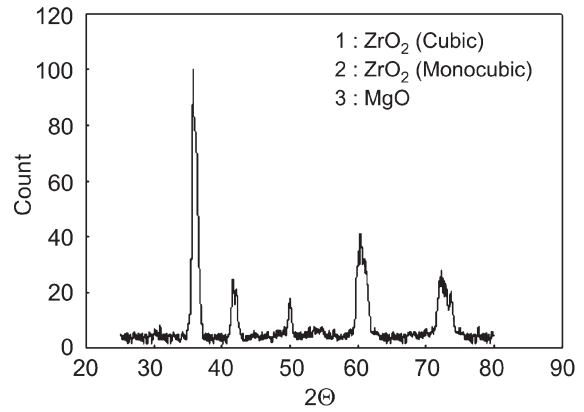


Fig. 5. XRD pattern of plasma sprayed coating.

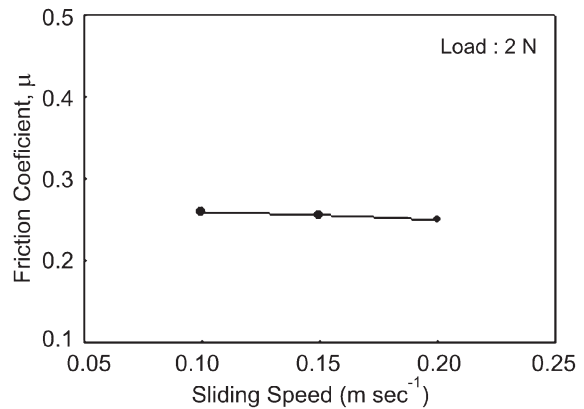


Fig. 6. Friction coefficient as a function of sliding speed.

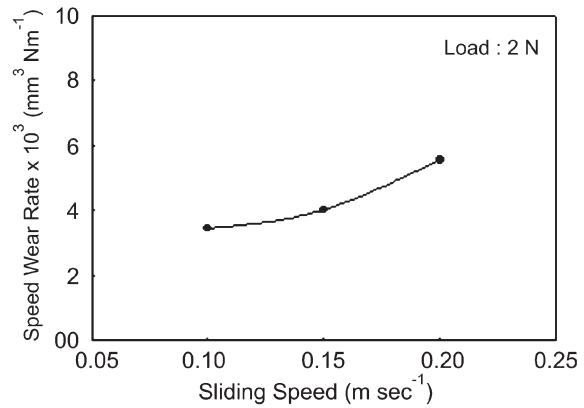


Fig. 7. Specific wear rate as a function of sliding speed.

metallic bond layer to cermet and from cermet to the ceramic layer as shown in Fig. 4a. The coating thickness was measured as 622.716 μm. The line-scan taken through coating was shown in Fig. 4b. The surface roughness values of obtained coatings were measured as average 6.771 μm. Microcracks and porosities on coating surfaces exist as seen in Fig. 4c. If the cross-

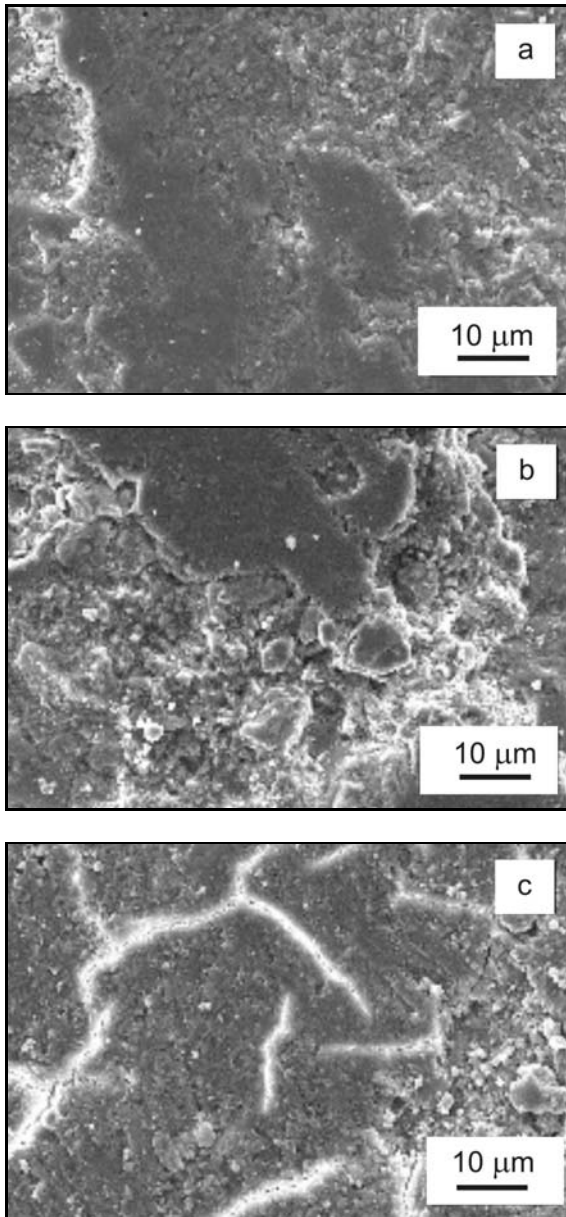


Fig. 8. Wear tracks morphologies of plasma-sprayed  $\text{MgZrO}_3$  coatings at (a) 0.1, (b) 0.15 and (c) 0.2  $\text{m s}^{-1}$  sliding speed.

-section micrographs of the plasma-sprayed coatings after polishing were examined, the oxides, porosity, unmelted and semi-melted particles would be seen. Furthermore, microcracks were found parallel to coating/substrate interface. All of these details are typical features of microstructure in the plasma sprayed coatings.  $\text{MgZrO}_3$  coatings deposited by plasma spraying consist of  $\text{MgO}$ , cubic and monoclinic  $\text{ZrO}_2$  phases as shown in Fig. 5.

The friction coefficients of plasma sprayed  $\text{MgZrO}_3$  coatings against WC-Co ball were realized using three different sliding speeds under a load of 2 N at ambient

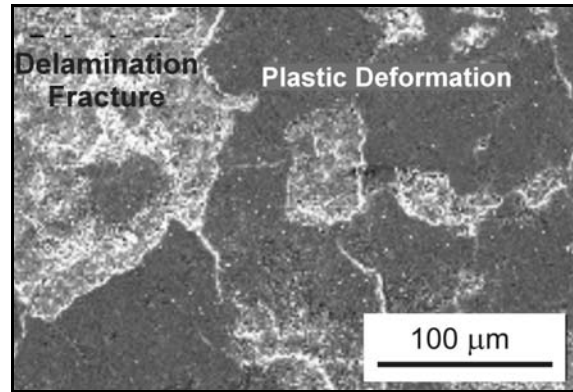


Fig. 9. Wear tracks morphologies of plasma sprayed  $\text{MgZrO}_3$  coatings at 0.15  $\text{m s}^{-1}$  sliding speed.

conditions (Fig. 6). It can be seen from Fig. 6, that the friction coefficient changes slightly with increasing sliding speed and decreases from 0.259 to 0.250 depending on sliding speed. Figure 7 represents the variation of specific wear rate versus applied sliding speed. The curve shows that the specific wear rates of samples increase with increasing sliding speed. The specific wear rate values rise from 3.447 to  $5.554 \times 10^{-3} \text{ mm}^3 \text{ N}^{-1} \text{ m}^{-1}$  with increasing sliding speed. This increment is almost two times greater than that of an original one.

SEM micrographs of the wear tracks on the plasma sprayed  $\text{MgZrO}_3$  coatings at different sliding speeds under the load of 2 N are shown in Fig. 8. The wear mechanism of these samples at 0.1 and 0.15  $\text{m s}^{-1}$  sliding speed is abrasive wear clearly presented on the worn surface as shown in Fig. 8a,b. The occurring of this mechanism is very natural because of surface roughness. It is attributed to its brittleness under low load. The debris resulting from prior brittle fracture acted as abrasive in following wear tests [13]. Wear tracks of worn surfaces on samples indicated plastic deformation occurred at some places and materials transfer. As a matter of fact the examination of wear tracks did not reveal an important difference between worn surfaces at the different sliding speeds. The single thing struck one's eyes is increasing microcracks on the wear tracks obtained at 0.2  $\text{m s}^{-1}$  sliding speed (Fig. 8c). The presence of microcracking on the coating surface causes excessive stresses and is attributed to fatigue fracture. These observed microcracks on the wear tracks disperse randomly and cause the delamination wear. As a result of delamination wear, the breakaways in the form of plate occur. The delamination wear is shown clearly in Fig. 9. It is noticed that wear debris obtained from coating and abrasive WC ball adhered to worn surface. Wear debris pile up mostly in cracks as shown clearly in Fig. 10.

EDS analysis was carried out on the wear tracks

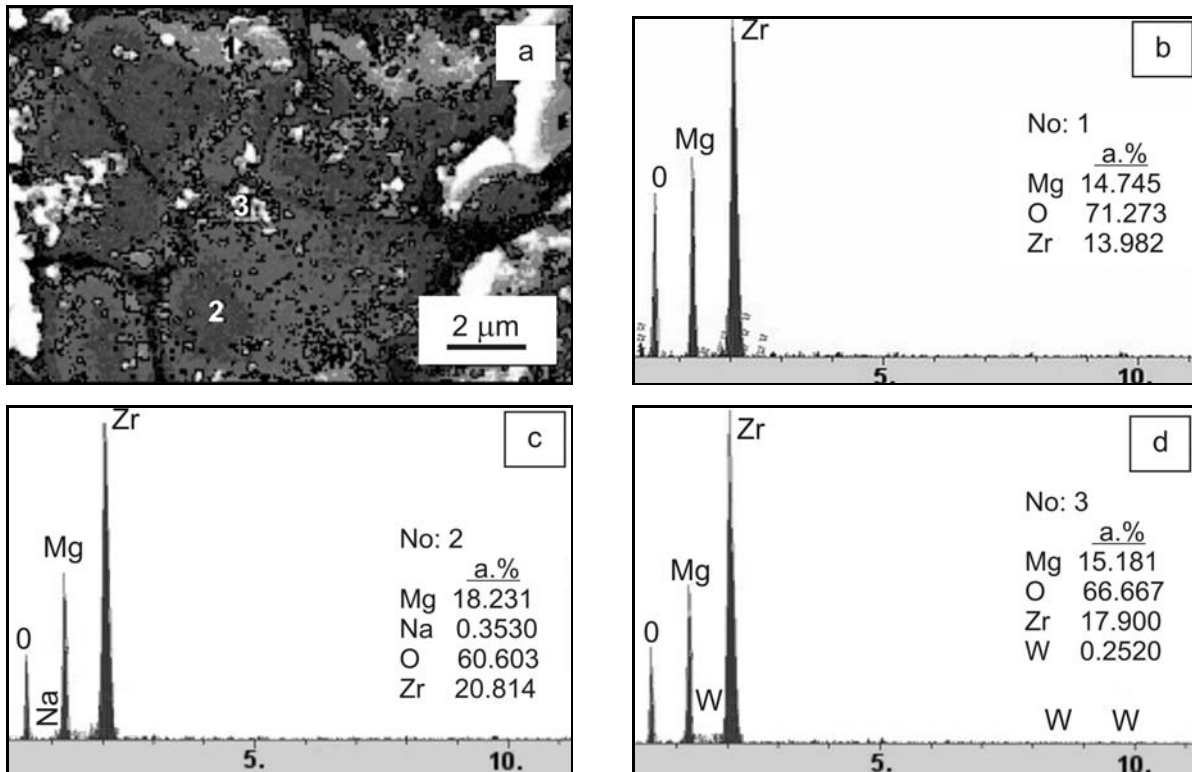


Fig. 10. SEM photos taken from different parts of worn surface (a), and their EDS spectra (b), (c), (d).

formed during wear test. EDS results are shown in Fig. 10. These results indicate that the particles formed on the wear tracks consist of Mg, Zr, O. Except for Mg, Zr, O, at the same time, W was also detected by EDS in analysis. This result reveals damage of WC ball during wear testing.

#### 4. Conclusions

It was shown that the specific wear rate of plasma sprayed  $\text{MgZrO}_3$  coatings of 304 L stainless steel increased with increasing sliding speed, while the friction coefficient changed slightly with increasing sliding speed. Although dominant wear mechanism was abrasive wear, the delamination wear and brittle fracture were also seen. The surface demonstrated plastic deformation. It seems some of the wear debris adhered on the surface. The adhered debris belongs to coatings and also WC balls. Microcracks were seen on the wear tracks. These microcracks increase and enlarge with increasing sliding speed. Then they connect with each other and break off in the form of plate. Consequently, these cracks cause the fatigue wear.

#### References

- [1] HUNTCHING, W. F.: Tribology, Friction and Wear of Engineering Materials. London, Adward Arnold 1992.
- [2] PERUGINI, G.: Thin Solid Films, 108, 1983, p. 415.
- [3] OHMORI, A.—AOKI, K.—SANO, S.—ARATA, Y.—IWAMOTO, N.: Thin Solid Films, 207, 1992, p. 153.
- [4] DEMIRKIRAN, A. Ş.—AVCI, E.: Surface and Coatings Technology, 116–119, 1999, p. 292.
- [5] WANG, Y.—JIANG, S.—WANG, M. et al.: Wear, 237, 2000, p. 176.
- [6] OUYANG, J. H.—SASAKI, S.—UMEDA, K.: Surface and Coatings Technology, 154, 2002, p. 131.
- [7] KVERNES, I.—LUGSCHEIDER, E.—LINDBLOM, Y.: In: Proceeding of 2<sup>nd</sup> European Symposium on Engineering Ceramics. Ed.: Riley, F. L. Norwell, Kluwer Academic Pub. 1989.
- [8] MAJUMDAR, D.—CHATTERJEE, D.: Thin Solid Films, 206, 1991, p. 349.
- [9] CHEN, H. C.—LIU, Z. Y.—CHUANG, Y. C.—XU, L. K.: Thin Solid Films, 232, 1993, p. 161.
- [10] TAYLOR, R.—BRANDON, J. R.: Surface and Coatings Technology, 50, 1992, p. 141.
- [11] HANNINK, R. H. J.—GROSS, V.—MUDDLE, B. C.: Ceramics International, 24, 1998, p. 45.
- [12] ESCHNAUER, H.: Surface Coatings, Thin Solid Films, 73, 1980, p. 1.
- [13] CHEN, H.—ZHANG, Y.—DING, C.: Wear, 253, 2002, p. 885.
- [14] SEN, U.—SEN, Ş.—YILMAZ, F.: Industrial Lubrication and Tribology, 57, 2005, p. 243.